Available online at www.sciencedirect.com

ScienceDirect

Physics Procedia 69 (2015) 530 – 536

Physics Procedia

10th World Conference on Neutron Radiography 5-10 October 2014

# Water and air redistribution within a dual permeability porous system investigated using neutron imaging

Jan Sacha* [1,2], Vladimira Jelinkova [2], Michal Snehota [1,2], Peter Vontobel [3], Jan Hovind [3] and Milena Cislerova [1]

*1 CTU in Prague, Faculty of Civil Eng., Dept. of Irrigation, Drainage and Landscape Engineering, Prague 166 29, Czech Republic*
*2 CTU in Prague, University Centre for Energy Efficient Buildings, Bustehrad 273 43, Czech Republic*
*3 Spallation Neutron Source Division, Paul Scherrer Institute, Villigen 5232, Switzerland*

**Abstract**

A ponded infiltration experiment was conducted under simultaneous imaging to investigate variations in quasi-saturated hydraulic conductivity a process frequently observed in infiltration experiments in soils with wide grain - size distribution. An artificially prepared heterogeneous sample composed of coarse quartz sand (representing pathways of preferential flow) and fine porous ceramic (representing soil matrix) was investigated. The sample was 34.5 mm high and 29.0 mm in diameter. Sequences of neutron radiography images (RI) of pixel size 0.045 × 0.045 mm were taken at one angle during particular transient phases of the flow process. During quasi-steady state flow stages of the experiment radiography images were acquired in range of angles 0-180° in 0.9° step and. 3D neutron tomograms (TI) were then developed. Using the data a quantitative evaluation of the spatial and temporal distribution of water content within the sample was conducted. For every RI and TI the amount of water in particular pixels and voxels, respectively, was calculated by subtracting the image of dry sample. The accuracy of the water content estimates derived from the images was checked by comparing them to the corresponding gravimetrically determined water content data. Heavy water with equilibrium air saturation was introduced into the sample during two recurrent infiltrations. Thirty five hours later, during second infiltration, the inflow was switched to degassed heavy water in order to remove residual air present in the sample. During the first twelve hours of first infiltration run flow rate through the sample decreased from 3.7 cm/hour to 1.0 cm/hour at the end of the "steady state flow" stage. The flow rate in second run decreased from 3.6 cm/hour to 1.6 cm/hour. Comparison of the tomogram of the sample at the beginning and one taken at the end of the steady state flow stage in each run shows an increase of water content in the porous ceramic, while the water content in the coarse sand decreased. On the contrary, during the subsequent infiltration with degassed water the flow rate increased to its maximum value of 10.5 cm/hour. The tomograms confirmed removal of the residual air during this stage. Increased water content in the coarse quartz sand was evident on a tomogram made at the end of the degassed water infiltration. The results show that the residual air saturation and its spatial distribution strongly affected the water flow in the quasi-saturated heterogeneous media representing natural soil.


Selection and peer-review under responsibility of Paul Scherrer Institut
doi:10.1016/j.phpro.2015.07.075

Selection and peer-review under responsibility of Paul Scherrer Institut

Keywords: neutron imaging (NI); ponded infiltration; preferential pathways; air redistribution; porous system; dual permeability

## 1. Introduction

**Nomenclature**

| | |
|---|---|
| $K_{QS}$ | quasi-saturated hydraulic conductivity |
| NI | neutron imaging |
| RI | radiography image (radiogram) |
| TI | tomography image (tomogram) |
| OB | open beam image |
| DC | dark current image |

Soil water dynamics in unsaturated and saturated zones in the subsurface may be significantly affected by accelerated flow along preferential pathways. These pathways may result from inhomogeneity of soil in combination with the presence of macropores. Preferential flow significantly alters the total hydraulic conductivity of soil. The most general method to describe systems with preferential pathways mathematically is incorporated in a dual permeability approach (e.g. Warren and Root (1963), Gerke and Van Genuchten (1993), Vogel et al. (2010)), however this approach doesn't account for the instability of saturated hydraulic conductivity observed in infiltration outflow experiments.

In the case of a fully saturated system, the saturated hydraulic conductivity $K_s$ is usually considered to be constant over time. Contrary to this assumption, decreases in $K_s$ over time have been observed in a number of "steady state" flow infiltration-outflow experiments. Snehota et al. (2014) have ascribed the decrease of steady state flow rate during ponded infiltration experiment to entrapped air redistribution between the fine soil matrix and preferential pathways. When air bubbles are present the soil cannot be fully saturated and therefore the term quasi-saturated hydraulic conductivity ($K_{QS}$) suggested by Faybishenko (1995) is more appropriate. Snehota et al. (2010) examined flow in a small undisturbed sample of coarse sandy loam classified as Dystric Cambisol using magnetic resonance imaging. They found that between two recurrent ponded experiments the steady flow rate decreased from 1.2 cm/hour to 0.3 cm/hour. Jelinkova et al. (2011) in a similar experiment on the same soil recorded a entrapped air related reduction of water flow rate from 10 cm/hour, when infiltration started into a dry soil sample, to 3 cm/hours when the recurrent infiltration started into the wet sample.

The process of coupled air and water flow within a soil sample can be studied using modern non-invasive visualization techniques like X-ray tomography (e.g. Hopmans et al., 1992) and magnetic resonance (MR) (e.g. Amin et al., 1993). Preferential flow has been investigated using MR imaging of the flow during recurrent infiltration-outflow experiments (e.g. Votrubova et al., 2003; Snehota et al., 2010). In the last decade neutron imaging has been employed as an innovative method for evaluating flow in soil. The imaging of water distribution in soil using neutrons was accomplished for example by Carminati et al. (2007), Vontobel et al. (2008) and Esser et al. (2010).

This paper is a follow-up to earlier research presented by Snehota et al. (2014). The aim of the research is to elucidate the character of flow in a composed sample trying to clarify the reasons for observed saturated hydraulic conductivity instability. The working hypothesis was that flow instability within the sample during ponded infiltration is due to residual air redistribution.

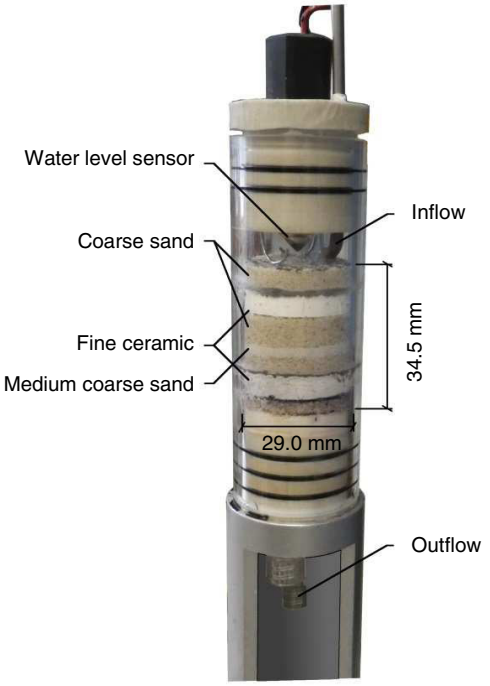


Fig. 1: Diagram of the sample

## 2. Methods

### *2.1 Ponded- infiltration experiment*

Ponded infiltration experiment was conducted on a heterogeneous porous sample. The sample was packed in axisymmetrical layers using three porous materials (fine ceramic, medium coarse sand and coarse sand) (Fig. 1). This design is analogous to natural soil systems with preferential pathways but with a simple, well-defined internal geometry.

The fine ceramic represents the region of slow water flow; the coarse sand represents the preferential pathways and the medium coarse sand simulates the narrow necks of the preferential pathways. The sample was packed in a quartz glass cylinder with inner diameter 29 mm and height 34.5 mm.

Digital peristaltic pumps (Reglo Digital 4 Channels, ISM 597 D, Ismatec®) supplied heavy water to the top of the sample. A constant level of ponding was maintained by the pump and a datalogger (CR3000, Campbell Scientific, Logan, Utah, U.S.A) by dosing a given quantity of water each time the water level sensor indicated a decrease of water level below a predefined level. The outflow was routed to a glass beaker. The inflow and outflow were continuously measured using digital balances connected to the datalogger using the RS232 communication protocol.

Two infiltration runs with non-degassed water were conducted. The first run lasted twelve hours, followed by an eight hour break with no infiltration. The second run lasted for twenty six hours and at the halfway point the infiltration was switched from aerated heavy water to the degassed heavy water.

### *2.2 Neutron imaging*

From the start of infiltration the sample was scanned using neutron radiography with an image resolution

of 1300 × 1500 pixels with pixel size 0.045 × 0.045 mm. The acquisition time of one radiogram was 10 s. The interval between shutter openings was 6 s.

Tomograms during the steady state flow stage were reconstructed from the sequence of radiograms. The sample was rotated 180°, in 201 steps of 0.9°. A total of 201 radiograms were acquired over approximately one hour to develop each tomogram.

Imaging was performed at NEUTRA beam line (Lehmann, et al., 2001) (http://www.psi.ch/sinq/neutra) of the PSI in Switzerland. The camera used was an ANDOR SOLIS SLL-071715 and the scintillator was a 75μm CAWP 062.

*2.3 Image processing*

The raw images had to be corrected (Kaestner et al., 2008; Schluter et al., 2014). Using images without sample (open beam) and images with closed beam shutter (dark current). The raw images were corrected for background noise, fluctuations of the neutron flux and spatial inhomogeneties of the neutron beam and the detector. The temporal inhomogeneties of the neutron beam were corrected using a rescale factor in order to set mean intensity value of the area outside the sample to equal one. Equation 1 details the correction of the raw images.

$$I_n = f\frac{I_{Raw} - I_{DC}}{I_{OB} - I_{DC}} \tag{1}$$

where $I_n$ (a.u.) is the normalized image, $f$ (-) is the rescale factor, $I_{Raw}$, $I_{DC}$ and $I_{OB}$ (a.u.) are the intensities of the raw image, the dark current image and the open beam image, respectively.

Thickness of water in the sample is then calculated in the direction perpendicular to the scintillator according to Carminati et al. (2007):

$$\Sigma_w d_w = \Sigma_{WET} d_{WET} - \Sigma_{DRY} d_{DRY} \tag{2}$$

where $\Sigma_w$, $\Sigma_{WET}$ and $\Sigma_{DRY}$ ($cm^{-1}$) is the attenuation coefficient of the water, the wet sample and the dry sample, respectively, $d_w$, $d_{WET}$ and $d_{DRY}$ (cm) is the thickness of the water, the wet and the dry sample, respectively.

An empirical correction for the beam hardening was used. The attenuation coefficient is linearly dependent on water thickness (Kang et al., 2013)

$$\Sigma = \Sigma_w + \beta d_w \tag{3}$$

where $\Sigma$ ($cm^{-1}$) is the total attenuation coefficient, $\Sigma_w$ ($cm^{-1}$) is the attenuation coefficient of water, $d_w$ (cm) is the thickness of water and $\beta$ ($cm^{-2}$) is the corrective parameter for the beam hardening.

The thickness of water is given by substituting equations 1, 2 and 3 into the Beer- Lambert law:

$$d_w = -\sqrt{\frac{-\ln\frac{I_{WET}}{I_{DRY}}}{\beta} + \left(\frac{\Sigma_w}{2\beta}\right)^2} - \frac{\Sigma_w}{2\beta} \tag{4}$$

The water volume in the image is given by:

$$V = \sum_{x=1}^{D}\sum_{y=1}^{H} d_w^{(x,y)} a^2 \tag{5}$$

where $V$ ($cm^3$) is the total water volume in the image, $d_w$ (cm) is the thickness of water, $a$ (cm) is the size of

pixel, *D* (px) is the width of the image and *H* (px) is the height of the image.

## 3. Results

The inflow and outflow flux rates were calculated from the weighed inflow and outflow. During the experiment a similar decrease of the flux rate was observed (Table 1) as in previous experiments done on natural soil (Snehota et al., 2014). The flux rate decreased from 3.7 cm/hour to 1.0 cm/hour during the first infiltration run and during the second infiltration run from 3.6 to 1.6 cm/hour before the application of degassed water, and then the flow rate increased slowly to 10.5 cm/hour.

Table 1: Overview of the flow rate and acquisition times of selected tomograms during the experiment

| Time since the start of infiltration (hour) | Description | Flux rate (cm/hour) | Tomogram no. |
|---|---|---|---|
| 0.5 | first infiltration - start of the quasi-steady state flow | 3.7 | - |
| 2.5 | 2.5 hours after the start of first infiltration | 1.3 | T1 |
| 10.2 | end of the first infiltration | 1.0 | T2 |
| 22.3 | second infiltration - start of the quasi-steady state flow | 3.6 | - |
| 23.5 | 2.1 hours after the start of second infiltration | 2.3 | T3 |
| 30.8 | before the degassed water application | 1.6 | T4 |
| 35.7 | 2.0 hours after the degassed water application | 2.0 | T5 |
| 45.7 | end of the second infiltration (steady state flow rate) | 10.5 | T6 |

The thickness of water layer (d) and the total attenuation coefficient (Σ) of the ponding were known. Based on this information $\Sigma_w$ and β from Eq. 3 were determined to fitting of these points ($\Sigma_w = 0.85$ cm$^{-1}$, $\beta = -0.094$ cm$^{-2}$).

The progress of the wetting front depicted in radiography images is shown in Fig. 2. The water volume estimates derived from these radiograms (according to Eq. 5) is compared with the weighed water volume calculated from digital balance records (Fig. 3).

From the selected tomograms the temporal and spatial changes of the attenuation coefficient were visualized (Fig. 4). The water content in the preferential pathways decreased during the steady state flow stage of each infiltration while it increased in the matrix. Significant increase in water content in the preferential pathways was observed after the application of degassed water.

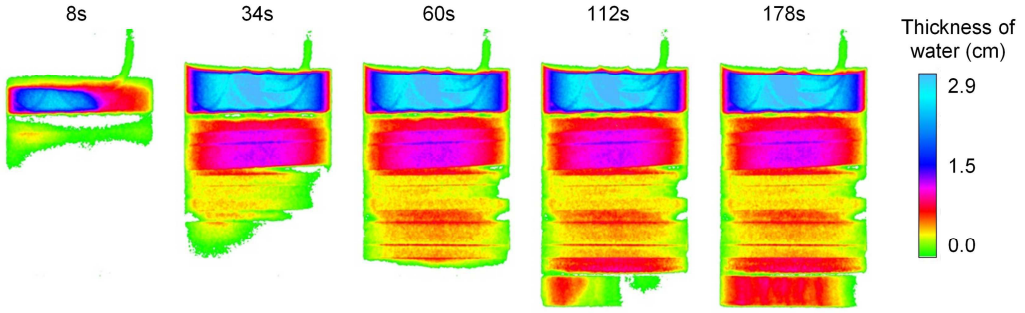


Fig. 2**:** A sequence of neutron radiography images illustrating the process of progress of the wetting front at the start of infiltration

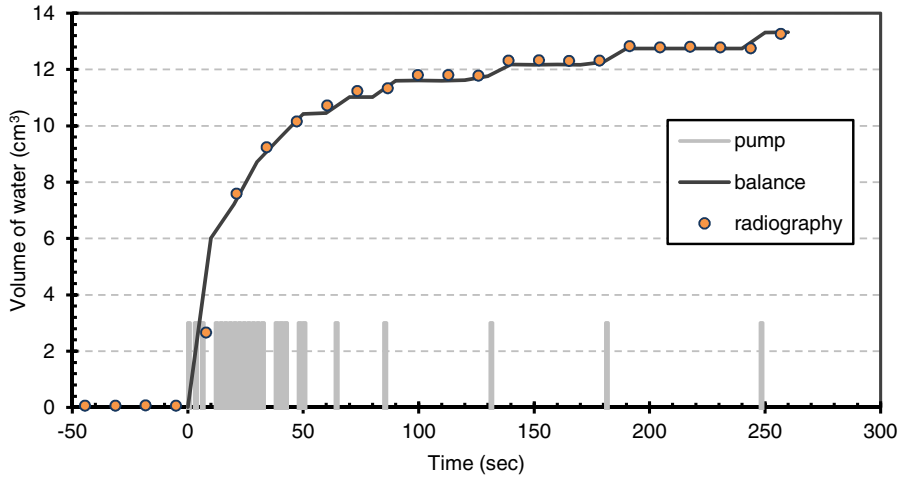


Fig. 3: Comparison of the volume of water added to the top of the sample (balance) and the amount of water in the sample derived from the images (radiography). Grey columns indicate the doses of water added to the sample.

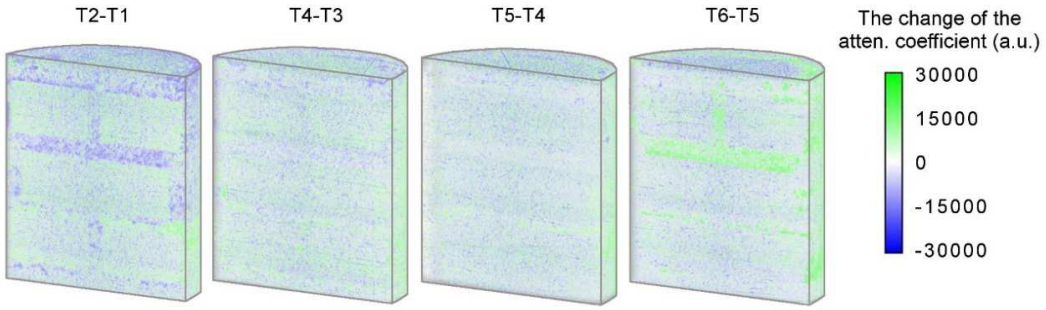


Fig. 4**:** Changes in the attenuation coefficient between the selected tomograms (see Tab. 1)

## 4. Conclusions

The tested hypothesis that the flow instability observed within the sample during ponded infiltration is due to the residual air redistribution has been supported by the experimental results. Quantitative data of water volume were obtained from neutron imaging at the very beginning of infiltration. The entrapped air redistribution was derived from changes in water content. Air bubbles appear to move gradually from the matrix to the preferential pathways where they accumulate in larger agglomerations forming a barrier to the preferential flow. On the contrary, the flux rate increased significantly after the application of degassed water when the air bubbles dissolved. This caused an increase in the water content which is clearly seen in comparing the different tomograms (Fig. 4). The results are in accordance with previous experiments performed on an artificial sample composed of three grades of sand (Snehota et al., 2014).

## Acknowledgements

Funding for this research was provided by the Czech Science Foundation (project No. 14-03691S) and Grant Agency of the Czech Technical University in Prague (grant No. SGS14/131/OHK1/2T/11).

This work is based on experiments performed at the Swiss Spallation Neutron Source SINQ, Paul Scherrer Institute, Villigen, Switzerland. This project has received funding from the European Union's Seventh Framework

Programme for research, technological development and demonstration under the NMI3-II Grant number 283883, SINQ 20131451.

## References

Amin, M.H.G., Chorley, R.J., Richards, K.S., Bache, B.W., Hall, L.D., Carpenter, T.A., (1993), Spatial and temporal mapping of water in soil by magnetic-resonance-imaging Hydrological Processes 7(3), 279-286.

Carminati, A., A. Kaestner, R. Hassanein, O. Ippisch, P. Vontobel, and H. Fluhler (2007), Infiltration through series of soil aggregates: Neutron radiography and modeling, Advances in Water Resources, 30(5), 1168-1178.

Esser, H. G., A. Carminati, P. Vontobel, E. H. Lehmann, and S. E. Oswald (2010), Neutron radiography and tomography of water distribution in the root zone, Journal of Plant Nutrition and Soil Science, 173(5), 757-764.

Faybishenko, B. A. (1995), Hydraulic behavior of quasi-saturated soils in the presence of entrapped air – laboratory experiments, Water Resources Research, 31(10), 2421-2435.

Gerke, H. H., and M. T. van Genuchten (1993), A dual-porosity for simulating the preferential movement of water and solutes in structured porous-media, Water Resources Research, 29(2), 305-319.

Hopmans, J.W., Vogel, T., Koblik, P.D. (1992), X-ray tomography of soil-water distribution in one-step outflow experiments. Soil Science Society of America Journal 56(2), 355-362.

Jelinkova, V., M. Snehota, A. Pohlmeier, D. van Dusschoten, and M. Cislerova (2011), Effects of entrapped residual air bubbles on tracer transport in heterogeneous soil: Magnetic resonance imaging study, Organic Geochemistry, 42(8), 991-998.

Kaestner, A., E. Lehmann, and M. Stampanoni (2008), Imaging and image processing in porous media research, Advances in Water Resources, 31(9), 1174-1187.

Kang, M., H. Z. Bilheux, S. Voisin, C. L. Cheng, E. Perfect, J. Horita, and J. M. Warren (2013), Water calibration measurements for neutron radiography: Application to water content quantification in porous media, Nuclear Instruments & Methods in Physics Research Section a-Accelerators Spectrometers Detectors and Associated Equipment, 708, 24-31.

Lehmann, E.H., Vontobel, P., Wiezel, L., 2001. Properties of the radiography facility NEUTRA at SINQ and its potential for use as european reference facility. Nondestructive Testing and Evaluation 16(2-6).

Schluter, S., A. Sheppard, K. Brown, and D. Wildenschild (2014), Image processing of multiphase images obtained via X- ray microtomography: A review, Water Resources Research, 50(4), 3615-3639.

Snehota, M., M. Cislerova, M. H. G. Amin, and L. D. Hall (2010), Tracing the Entrapped Air in Heterogeneous Soil by Means of Magnetic Resonance Imaging, Vadose Zone Journal, 9(2), 373-384.

Snehota, M., Jelinkova, V., Sobotkova, M., Sacha, J., Vontobel, P., Hovind, J., (2014) Three-dimensional visualization and quantification of the water and entrapped air redistribution in soil by neutron imaging. Water Resources Research (In review)

Snehota, M., Jelinkova, V., Sacha, J., Frycova, M., Cislerova, M., Vontobel, P., Hovind, J., (2014) Experimental investigation of preferential flow in near-saturated intact soil sample Physics Procedia (in this issue)

Vontobel, P., R. Hassanein, A. Carminati, A. Kaestner, P. Lehmann, and A. Koliji (2008), Neutron Imaging for Soil Physics and Geology, 369-373 pp.

Votrubova, J., M. Cislerova, M. H. G. Amin, and L. D. Hall (2003), Recurrent ponded infiltration into structured soil: A magnetic resonance imaging study, Water Resources Research, 39(12).

Warren, J. E., and P. J. Root (1963), The behavior of naturally fractured reservoirs, Society of Petroleum Engineers Journal, 3(3), 245-255.